JACS
JOURNAL OF THE AMERICAN CHEMICAL SOCIETY

ARTICLE

pubs.acs.org/JACS

Probing Ground-State Single-Electron Self-Exchange across a Molecule−Metal Interface

Yuanmin Wang, Papatya C. Sevinc, Yufan He, and H. Peter Lu*

Department of Chemistry, Center for Photochemical Sciences, Bowling Green State University, Bowling Green, Ohio 43403, United States

Supporting Information

ABSTRACT: We have probed single-molecule redox reaction dynamics of hemin (chloride) adsorbed on Ag nanoparticle surfaces by single-molecule surface-enhanced Raman spectroscopy (SMSERS) combined with spectroelectrochemistry. Redox reaction at the molecule/Ag interface is identified and probed by the prominent fluctuations of the Raman frequency of a specific vibrational mode, ν_4, which is a typical marker of the redox state of the iron center in a hemin molecule. On the basis of the autocorrelation and cross-correlation analysis of the single-molecule Raman spectral trajectories and the control measurements of single-molecule spectroelectochemistry and electrochemical STM, we suggest that the single-molecule redox reaction dynamics at the hemin−Ag interface is primarily driven by thermal fluctuations. The spontaneous fluctuation dynamics of the single-molecule redox reaction is measured under no external electric potential across the molecule−metal interfaces, which provides a novel and unique approach to characterize the interfacial electron transfer at the molecule−metal interfaces. Our demonstrated approaches are powerful for obtaining molecular coupling and dynamics involved in interfacial electron transfer processes. The new information obtained is critical for a further understanding, design, and manipulation of the charge transfer processes at the molecule−metal interface or metal−molecule−metal junctions, which are fundamental elements in single-molecule electronics, catalysis, and solar energy conversion.

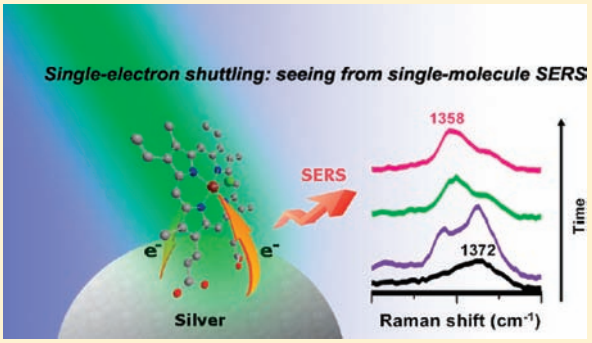

INTRODUCTION

Redox reactions, i.e., reduction−oxidation reactions, widely exist and are playing important roles in chemistry, biology, technology, and industry. For a redox reaction, the key processes are the electron transfer (ET) between the reductant and oxidant and subsequently produce the reduced states or oxidized states of chemical species. Therefore, electron transfer dynamics is the core of the redox reaction dynamics. In ensemble-averaged experiments, redox reaction dynamics has been widely investigated in electrochemistry,[1,2] catalysis,[3−7] biosensor and bioelectronics,[8] and cellular respiration.[9,10] At the single-molecule level, with the developments of the molecular electronics research, most of the investigations on redox reaction dynamics focus on molecule−metal interfaces or metal−molecule−metal junctions.[11−23] For single-molecule electronics, the main challenge for its commercialization is the difficulty to connect the molecular sized circuit to bulk electrodes in a molecule-level reproducible way for mass production. Therefore, it is critical to obtain a fundamental and molecule-level understanding of the molecule−metal interfaces or metal−molecule−metal junctions.

Electron transport properties of a molecule in a interstitial metal nanogap have been demonstrated to strongly depend on the electronic coupling between the molecule and electrode. Different conducting performance can be observed depending on the strength of the coupling.[12] Accordingly, conductance fluctuation has been observed for a single polyaniline strand sandwiched in a metal nanogap. At the redox formal potential, the conductance fluctuates between the reduced and oxidized states recorded in a current−time trajectory. However, the probability for the molecule to stay in the oxidized state is high when the gate voltage is far greater than the formal redox potential.[24] Similar fluctuations have also been observed in other metal−molecule−metal junctions and also proposed to be the origin of common $1/f$ noise in electronic devices.[13,23] For a metal−molecule−metal junction, current-induced metal-atom motions, molecular conformation changes, and chemical bond fluctuations have been suggested to be the chemical and mechanical reasons for the fluctuations.[13,23] On the other hand, the fluctuation of the conductance in a single molecule−metal junction is coincident with the fluctuation and inhomogeneity of the single-molecule dynamics.[25−28]

In our previous work, single-molecule fluctuation dynamics have been investigated by fluorescence spectroscopy, photon-stamping, and Raman spectroscopy.[27,29−37] At the single-molecule

Received: October 15, 2010
Published: April 12, 2011

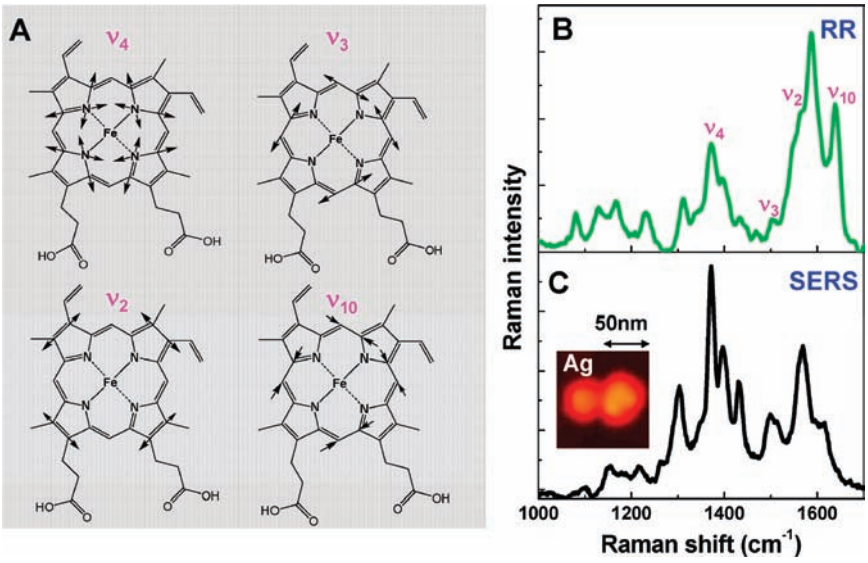

Figure 1. Typical vibrational modes and Raman spectra of hemin. (A) Diagram illustrating four characteristic vibrational modes of the porphyrin skeletal structures of hemin (or Heme). (B and C) Typical resonance Raman spectrum and single-molecule SERS of hemin, respectively. A SEM image of a Raman-active dimer of Ag NPs is shown in the inset of C.

level, the interfacial electron transfer dynamics at the molecule–TiO_2 nanoparticle (NP) interfaces has been demonstrated to be intermittent and inhomogeneous.[33−35] The fluctuation of the single-molecule ET dynamics has been suggested to be regulated by the molecule–semiconductor interactions, such as the driving force of free energy gap between the excited state of molecule and the conduction band of TiO_2 semiconductor, the vibrational relaxation energy of the adsorbed molecules and the surface vibrational modes of TiO_2, and the electronic coupling between the molecules and the TiO_2, etc. The intermittent ET dynamics, which was also observed later by other groups for various interfacial electron transfer systems,[38−40] is most likely a general phenomenon for a single molecule adsorbed on a semiconductor surface since thermal fluctuations typically perturb the molecule–substrate interaction energetics at room temperature.[41] In this article, we report the fluctuation dynamics of the single-molecule redox reaction at the molecule–metal interface, which is revealed by single-molecule surface-enhanced Raman spectroscopy (SMSERS) as well as single-molecule spectroelectrochemistry. On the basis of the autocorrelation and cross-correlation function analysis of the Raman spectrum-mean trajectories, we suggest that the single-molecule redox reaction at the hemin–Ag interface is mainly spontaneous and driven by thermal fluctuations, although we cannot rule out the existence of a minor photoinduced fluctuation component. In previous reports, such as on molecular electronics, high electric fields were typically applied across the molecule–substrate interfaces, and the electric conductance fluctuation dynamics was demonstrated to be an electric current-induced effect. However, the fluctuation dynamics revealed here is a real-time picture of a single-electron self-exchange across a molecule–metal interface without a biased external electric field. Therefore, our unique experimental approaches provide critical and fundamental characterization and analyses for the single-molecule electronics, especially for the further understanding, design, and manipulation of the interfacial electron transfer dynamics at the molecule–metal interfaces or metal–molecule–metal junctions.

EXPERIMENTAL SECTION

Materials and Sample Preparation. Hemin chloride, $AgNO_3$, sodium citrate, and poly-L-lysine are purchased from Sigma Aldrich and used as received. Silver nanoparticles are synthesized by citrate reduction of $AgNO_3$ according to the Lee–Meisel method.[42] NaCl is added to the Ag NP solution as an activation component for SERS measurements. The average size of the Ag NP is ~50 nm as identified by SEM. One typical Ag NP dimer is shown in Figure 1B inset, and a strong electromagnetic field typically exists at the interstitial site of the nanoparticle dimer under laser excitation.[43−45] For SMSERS measurements, hemin in aqueous solution is diluted to 1.4×10^{-9} M or 4.8×10^{-11} M. Poly-L-lysine is used to immobilize Ag NPs on the coverslip.

Surface-Enhanced Raman Measurements, Spectroelectrochemistry, and Electrochemical Scanning Tunneling Microscopy (STM). Single-molecule SERS and imaging are recorded by an Axiovert 135 inverted scanning confocal microscope, equipped with a 100 × 1.3 NA oil immersion objective (Zeiss FLUAR). A continuous-wave (CW) laser (532 nm, CrystaLaser) is used to pump the sample at 3 μW for SERS and 60 μW for resonance Raman measurements. A beam splitter Z532rdc (Chroma) is used to reflect the excitation light into the microscope objective. Before the scatted light focusing into a monochromator (Triax 550, Jobin Yvon), a band-pass filter HQ580/60 M is positioned before the entrance slit to further reject the Rayleigh light. The Raman spectra are collected by a LN CCD (Princeton Instruments) cooled at about −100 °C with a resolution of 2 cm^{-1}. The setup is carefully calibrated using mercury lamp and cyclohexane (mode at 801.3 cm^{-1}) before the Raman measurements. The electrochemistry is performed by a CHI 600C electrochemical workstation, which is equipped with a homemade cell and a three-electrode system (working electrode: ITO/glass coverslip; counter electrode: platinum wire; reference electrode: silver wire). A solution of 0.1 M NaCl is used as supporting electrolyte. Before the Raman measurements, cyclic voltammetry is first performed, and then the potential is applied at a more negative or positive value than the formal redox potential to keep the molecules at reduced state or oxidized state, respectively. As a control experiment, the electrochemical STM imaging measurement was performed at the Au(111)–0.1 M H_2SO_4 interface by using a STM high resolution scanner (Agilent 5500 SPM Microscope, Agilent Technologies).

RESULTS AND DISCUSSION

As a high-spin five-coordinate Fe(III) compound, hemin is a model molecule to probe the redox reaction at molecule−metal interfaces by using SERS.[46−50] So far, the redox reaction at the hemin−metal interface has been observed at both ensemble and single-molecule level. However, the detailed charge-transfer dynamics as well as the inherent nature of the mechanism of the redox reaction have not been revealed yet. On the basis of literature,[51,52] several vibrational modes of hemin such as ν_4, ν_3, ν_2, and ν_{10} are typical markers of the porphyrin core size and the iron electronic structure. A schematic description of these four vibrational modes is shown in Figure 1A. The ν_4 mode is the marker of iron oxidation state, and its vibrational frequency is in a range of ∼1368−1377 cm^{-1} for the ferric (Fe(III)) state and ∼1344−1364 cm^{-1} for the ferrous (Fe(II)) state.[51] For the ν_3 mode, it is sensitive to the coordination and spin state. Its vibrational frequency is in a range of 1470−1480 cm^{-1} for the six-coordinated high-spin hemin, 1490−1500 cm^{-1} for the five-coordinated high-spin hemin, and 1500−1511 cm^{-1} for the six-coordinated low-spin hemin.[51] Figure 1B and 1C shows the resonance Raman (RR) and a typical SMSERS of hemin. Apparently, the two spectra have a similar profile, and the typical vibrational modes such as ν_4, ν_3, ν_2, and ν_{10} are all well resolved. As the iron oxidation state marker, ν_4 peaks occur at 1373 and 1372 cm^{-1} in the RR and SMSERS spectra, respectively, which indicates that hemin is in the oxidized state. In the SMSERS measurements of hemin of 1.4×10^{-9} M or 4.8×10^{-11} M, we observed spectral fluctuations, blinking, and final quantized single-step photobleaches of the Raman spectra, the typical signatures of measurements at the single-molecule detection limit, although we cannot rule out the possibility that some observed hot spots may contain multiple molecules. One set of the time-dependent SMSERS recorded from a single hot spot is shown in Figure 2. SMSERS[43,45,53−64] is an ultrasensitive approach to detect individual molecules by probing its vibrational fingerprint. Compared with ensemble measurements, the typical characteristics of the SMSERS are the fluctuations of vibrational frequency and intensity as well as the relatively narrowed Raman peaks.[59,65−67] The origin of the fluctuations have been attributed to the interaction changes and fluctuations at the molecule−substrate interface,[31,65,67−70] thermal effect,[59,71,72] and isotopic effects.[67] The interaction fluctuations include surface work function fluctuation of substrates, electron transfer occurrences, molecule motions, and conformational changes. In Figure 2A, four spectra are shown as a zoom-in view of a spectral fluctuation trajectory (Figure 2B) to illuminate the spectra fluctuation evolution profile of vibrational mode ν_4, the oxidation state marker of the iron center. Obviously, with a time scale of about 80 s, the ν_4 peak shifts from 1372 to 1358 cm^{-1}, which indicates that the hemin molecule shifts from the oxidized state to the reduced state, considering that the frequency of ν_4 has been reported in a range of ∼1368−1377 cm^{-1} for the ferric state and ∼1344−1364 cm^{-1} for the ferrous state.[51]

To get more information about the redox reaction at the hemin−Ag interface, on the basis of the data in Figure 2, we chose modes ν_4 and ν_3, which are sensitive to the redox state change and according molecular structure changes, to calculate the Raman spectrum mean trajectories (Figure 3A). Unambiguously, both ν_4 and ν_3 peaks show strong fluctuation with averaged amplitudes ∼10 to 15 cm^{-1}. As the iron oxidation state marker, ν_4 clearly fluctuates between oxidized state and reduced state and also presents possible intermediate states. Here, the intermediate

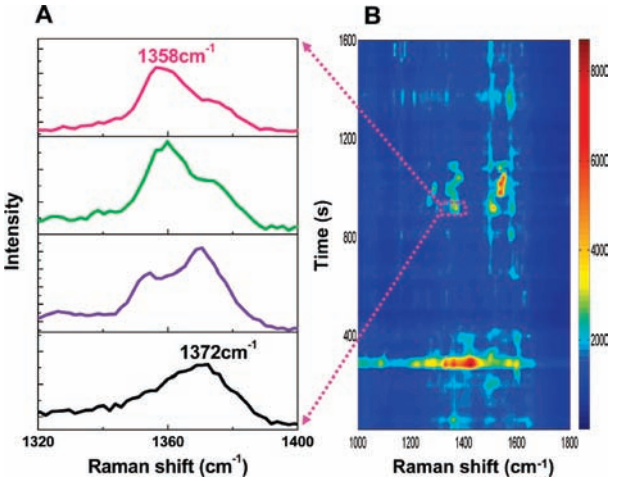

Figure 2. (A) Four consecutive spectra, which show the evolution of ν_4 from the oxidized state to the reduced state, are shown as a zoom-in view. (B) Time-dependent SERS spectra of hemin (1.4 nM) adsorbed on Ag NP surfaces. Typical vibrational modes, ν_4, ν_3, ν_2, and ν_{10}, are prominent but show strong fluctuation at the single-molecule level.

states refer to the states where the charge is just polarized or partially transferred at the molecule−metal interface.[73]

At the molecule−metal interface, charge transfer events are typically complex. For a molecule−metal junction, due to the induced dipole at the interface, charge delocalization and vibrational reorganization can occur at the nanocontact.[74,75] For example, electron transfer at the Cu(100)/tetracyano-*p*-quinodimethane (electron acceptor) interface leads to substantial structural rearrangements on both the organic and metallic sides.[76] The charge transfer at the molecule−metal interface has been identified to be originated from subtle and complex cumulative effects of (i) metal to molecule charge transfer, (ii) back charge transfer from molecule to metal, which results from a strong hybridization of deep-lying occupied molecular orbitals, and (iii) strong geometric distortions of the molecule.[77] It has also been demonstrated that the Ag substrate contributes to the lowest unoccupied molecular orbital (LUMO) of 3,4,9,10-perylene-tetracarboxylic acid dianhydride (PTCDA), and the metal−molecule hybrid character was proved at the PTCDA−Ag interface.[78]

For the hemin−Ag system, the charge transfer is evidenced by the fluctuation profile of ν_4 (Figure 3A). The spectrum mean trajectories record the single electron-transfer events between hemin molecule and silver NP surface. The charge transfer at the hemin−Ag interface revealed by our SMSERS measurements is consistent with the results from previously reported ensemble-averaged SERS measurements:[79] For example, a partial electron transfer from the Ag surface to the heme group (an analogue of hemin) of protein oxyhemoglobin was identified by observing a Raman vibrational mode ν_4 frequency decrease of 5 cm^{-1} from RR to SERS.[79]

To probe the single-molecule charge transfer dynamics at the hemin−Ag interface, we have analyzed the fluctuation trajectories of vibrational mode ν_4 and ν_3 by calculating the auto-correlation function (ACF) from the Raman spectral mean trajectories (Figure 3B and 3C). The fluctuation constants of the correlation functions are deduced to be 0.033 ± 0.001 and 0.038 ± 0.001 s^{-1}, respectively. This is consistent with the previously reported slow fluctuation of the SMSERS.[65,69] We

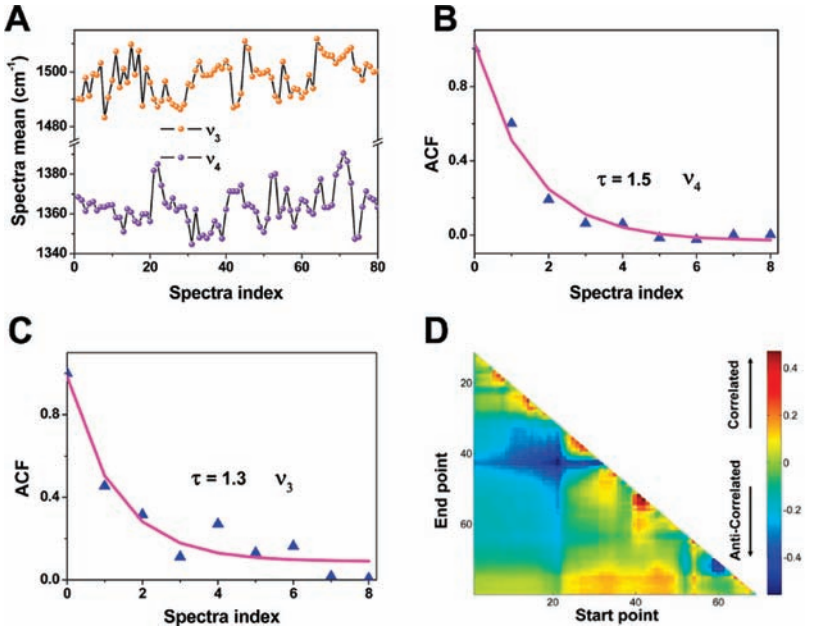

Figure 3. Statistical analysis of Raman spectra mean of oxidation state marker ν_4 and spin and coordination marker ν_3. (A) Raman spectra mean fluctuation profile of mode ν_4 and ν_3 for 80 consecutive spectra. Here, we use 20 s/spectrum as the optimized integration time to decrease the possibilities of Raman blinking for the subsequent correlation analysis and obtaining the charge transfer dynamics. (B and C) Autocorrelation function decay profiles of spectrum mean trajectories of ν_4 and ν_3; the fluctuation constants are deduced to be 1.5 and 1.3, respectively. (D) 2D-cross-correlation mapping of the spectrum mean trajectories of ν_4 and ν_3 for the 80 Raman spectra. Obviously, the fluctuation of ν_4 and ν_3 is correlated or anticorrelated from time to time, implying that the inhomogeneous spin states (or coordination) change during the redox reaction.

also carried out a 2D regional cross-correlation analysis[80] between ν_4 and ν_3 (Figure 3D), and we observed that, with ν_4 fluctuating between two redox states, ν_3 shows correlation or anticorrelation with ν_4. Previously, ensemble-averaged SERS measurements of hemin indicated complex correlation between ν_4 and ν_3.[46,48] The complexity is due to the different spin states and coordination of Fe(II) products under different experimental conditions. In our single-molecule measurements, we observed that the correlation between ν_4 and ν_3 fluctuates with time, which reflects the structural changes (such as spin states and coordination changes) during the redox reaction, although we cannot rule out some possibilities of the nanoscale gradient-field perturbation effect.[81] Nevertheless, both modes are sensitive to the redox state changes of the single hemin molecules. On the other hand, the correlation or anticorrelation analyses reveal more detailed information such as rate of the redox reaction. The correlation or anticorrelation of two specific modes, which are the oxidation state marker and the spin state (and coordination) marker, most likely reflects the real rate of the redox reaction. The fluctuation profile of ν_3 could be a response in molecular structure or conformational changes to the oxidation state change. We calculate the 1D cross-correlation of the first 50 spectra. A well-defined cross-correlation function (see Supporting Information, Figure S1) is obtained, and the decay rate is fitted to be 0.011 s^{-1}, which is much slower than the fluctuation rate of ν_4 (0.033 s^{-1}) or ν_3 (0.038 s^{-1}) alone. This is because some fluctuation events in the ν_4 or ν_3 trajectory most likely involve partial charge transfer (or charge reorganization) events but not complete charge transfer events. For an electron to transfer completely across the interface, more activation energy is needed compared with the charge delocalization or polarization process. From the reaction rate, we estimate that a single charge-transfer event rate constant is about 0.011 s^{-1} (i.e., the time scale is about 90 s for a single ET event). Coincidently, this rate also can be directly observed from the zoom-in view in Figure 2A. According to the Arrhenius equation (eq 1):

$$k = A \exp(-E_a/RT) \quad (1)$$

where k is the rate constant, A is the pre-exponential factor, E_a is the activation energy, R is the constant, and T is absolute temperature. Taking the pre-exponential factor (A) with a normal range ($10^{10}-10^{13}$ s^{-1}), we get the activation energy in a range of 68.2−85.3 kJ/mol, i.e., 0.7 to 0.8 eV for the redox reaction at the hemin−Ag interface. This value is close to the reported 0.3 to 0.5 eV for one-electron transfer from the Fermi level of the aluminum surface to the adsorbed oxygen molecule.[82] There is also a possibility that oxidation of the Ag NP surfaces, from exposure to the air, may raise the actual surface work function energy of the hemin−Ag interfaces. Furthermore, the Ag NP surface is highly heterogeneous at nanoscale, and there must be a significant inhomogeneity of the surface work function energy distribution, which supports a qualitative but not necessarily quantitative comparison of the Ag surface work function energy to the interfacial self-exchange electron transfer activation energy.

Single-molecule spectroelectrochemistry is an effective technique to probe the redox states of molecules.[83−85] As a control measurement, the single-molecule redox reaction at the hemin−Ag interface is further evaluated by the spectroelectrochemistry correlated with SMSERS measurements (The typical setup is shown in Figure 4A). On the basis of the ensemble-averaged cyclic voltammogram (Figure 4B), an overpotential of 0.5 or −0.5 V, which is far beyond the redox formal potential of hemin, is applied in the single-molecule experiments to keep a hemin molecule in the oxidized state or reduced state, respectively. Figure 4C shows two single-molecule Raman spectral mean

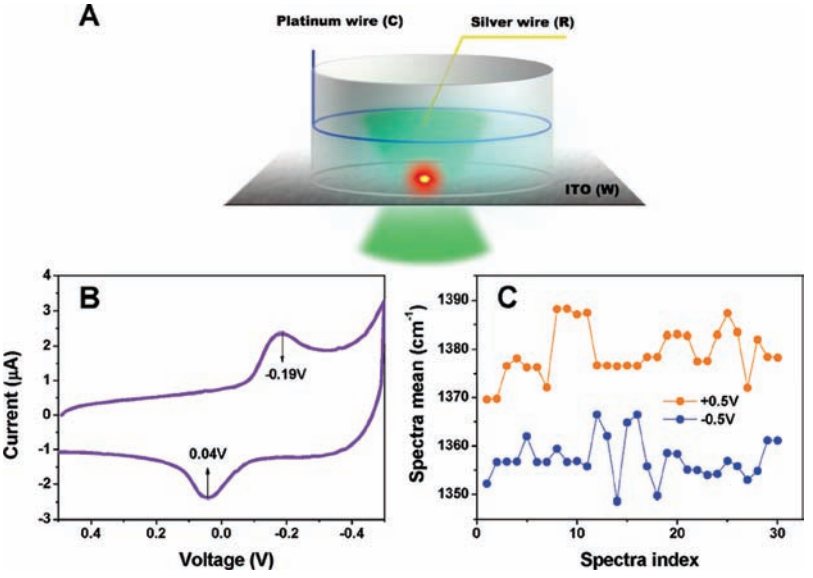

Figure 4. (A) Schematic of the homemade electrochemical cell coupled with confocal Raman microscopy. (B) Cyclic voltammogram of 0.43 μM hemin molecules adsorbed on the Ag NP-coupled ITO surface. (C) Fluctuation profiles of the Raman spectral mean of mode ν_4 under +0.5 V and −0.5 V at the single-molecule level. The applied potentials are enough to keep the single hemin molecule in an oxidized state or reduced state. Although the frequency still shows fluctuation in both cases, it indicates the dominant states.

trajectories of vibrational mode ν_4 under reverse potential. Apparently, at the single-molecule level, the hemin molecule can sense the positive or negative electric field and shows a high probability to stay in an oxidized or reduced state, respectively. This observation is consistent with the ensemble-averaged measurements that indicate that ν_4 shifts from 1370 cm^{-1} to 1360 cm^{-1} when the hemin molecules are reduced under the negative overpotential.[46] Nevertheless, we observed significant fluctuations of the redox state self-exchanges of single-molecule hemin on the Ag NP surface by the Raman spectral mean trajectories under either positive or negative overpotentials, i.e., single-molecule hemins have a measurable probability of switching to the opposite redox state, although the single-molecule hemin stays predominately in a redox state under a specific overpotential. We calculate the probability distribution of the single-molecule Raman spectral means of mode ν_4 under +0.5 V, −0.5 V, and 0.0 V overpotentials (Figure 5). For both cases of with and without overpotential control, the Raman mean distributions are Gaussian-like. Under the overpotential of 0.5 (−0.5) V, the distribution is dominated by the oxidized or reduced state, evidenced by the first moment of the distribution being ∼1375 or 1357 cm^{-1}, respectively. For the case of without potential control, the first moment of the distribution is ∼1365 cm^{-1}, which implies that neither oxidized or reduced state is dominant, and that the single molecule fluctuates between oxidized states, reduced states, and possible intermediate states, i.e., electron partially transferred or polarized states. Consequently, the distribution only shows one peak.

Fluctuation dynamics of the SMSERS, in recent years, has been extensively studied for various systems, and the origin of the fluctuation has been attributed to the interaction changes and fluctuations at the molecule−substrate interface,[31,65,67−70] thermal effect,[59,71] and isotopic effects.[67] The interaction fluctuations, as we have mentioned previously, include surface work function fluctuation of substrates, electron transfer occurrences, molecule motions, and conformational changes. If the isotopic

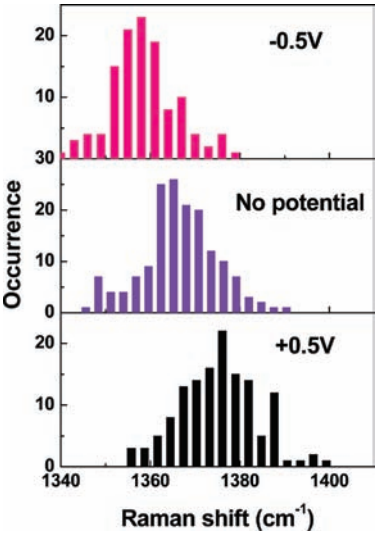

Figure 5. Probability distributions for the spectra mean of mode ν_4 with and without potential at the single-molecule level. The clearly observed frequency shift indicates the dominant oxidation state of the single hemin molecules.

effect is treated as a rare and special event, we suggest that the most common and primary driving force of the fluctuation is the thermal effect because all the interaction changes at the molecule−metal interface could be driven by thermal fluctuation under our experimental conditions. It has been demonstrated that the strong spectral fluctuation at hot spots could be effectively eliminated by lowering the local temperature of the samples to generate very stable Raman spectra for the nonbonding molecules.[71] Also, thermally induced orientation and chemistry are proved to be the root cause of the single-molecule Raman blinking.[59] On the basis of the above demonstrations, our understanding, and our control experiment (see Supporting

dx.doi.org/10.1021/ja109306r |J. Am. Chem. Soc. 2011, 133, 6989–6996

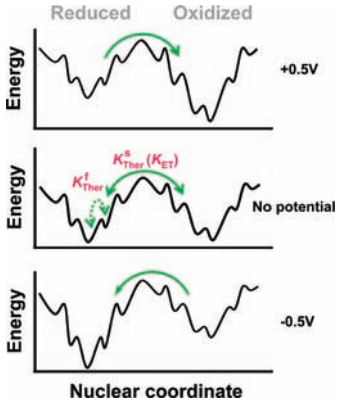

Figure 6. The potential energy surface schematic illustration of the single-molecule redox reaction under different conditions. K^{f}_{ther}: fast thermal fluctuation rate; K^{s}_{ther}: slow thermal fluctuation rate; K_{ET}: ET rate at the hemin−Ag interface. Without potential, the redox reaction is mainly driven by the slow thermal fluctuation. Therefore, $K_{ET} \approx K^{s}_{ther}$. If potential is applied, the redox reaction is dominated by one direction because of the activation barrier difference.

Information, Figure S2), we propose a model to describe the thermally induced single-molecule redox reaction at the molecule−metal interface (Figure 6). From the autocorrelation and cross-correlation analyses, we suggest that two kinds of thermal effects, including a fast component (deduced from autocorrelation function) and a slow component (deduced from correlation function), are the main driving forces of the fluctuation dynamics of the hemin−Ag NP system. The redox reaction could be driven by the slow thermal fluctuation but is perturbed by the fast fluctuation (Figure 6). Without potential control, the hemin molecule shows jumping between reduced state and oxidized state as observed from the experimental data in Figure 3A. With potential control (such as 0.5 V and −0.5 V), the hemin molecule will show more possibility to stay in the oxidized state or reduced state due to the tilted energy barrier. We suggest that the fast component of the thermal effect, which is shown as small wiggling on the surface potential, is the driving force for the spectra mean shift of several wavenumbers, and physically it only induces the polarization of the charge or partial charge transfer at the molecule−metal interface. Furthermore, the slow component of the thermal effect, which is shown as large wiggling on the surface potential, is the driving force for a complete charge transfer event between Ag and the hemin molecule. It is shown as a large shift (at least 10 cm^{-1}) in the Raman spectra mean in Figure 3A. The suggestion of thermally induced single-electron charge transfer at the hemin−Ag interface is also consistent with the ensemble-averaged measurements of the interfacial ET study of heme proteins, in which the thermal fluctuation is demonstrated to be the main factor that determines the ET rates.[86] Moreover, our results can also be supported by a theoretical study which indicates charge fluctuations at the molecule−metal interface even without biased potential.[87]

The ground-state charge transfer at the hemin−Ag interface described here is different from the charge-transfer enhancement factor in SERS. According to a unified expression of SERS,[88] surface plasmon resonance, charge-transfer resonance at the metal−molecule interface, and an allowed molecule resonance contribute to the polarizability tensor of the molecule−metal system. As in the Herzberg−Teller effect, charge-transfer resonance at the metal−molecule interface means vibronic coupling

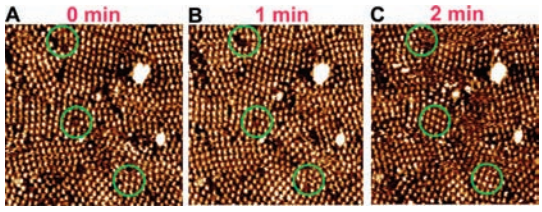

Figure 7. The thermally driven redox reaction of single Co(II)Pc molecules at the Au (111) surface with a reduction potential of 0.1 V vs SCE at (A) 0 min, (B) 1 min, (C) 2 min. The fluctuation of the brightness of a single molecule indicates the oxidation state changes.

and electron exchange between the metallic excited states and lowest unoccupied molecular orbital (LUMO) under laser illumination. The "hot" excited metallic electrons oscillate at the metal−molecule interface and can only stay at the anion surface potential surface for several femtoseconds.[89] Therefore, this charge-transfer term in SERS enhancement involves an excited state and electronic transient process without nuclear coordinate change. It is clearly different from the ground-state charge transfer events at the hemin−Ag interfaces that can be time-resolved on a seconds time scale and are involved in significant nuclear coordinate changes. Furthermore, the demonstrated ground-state charge transfer events naturally exist at the hemin−Ag interfaces (This can also be evidenced by the ground-state electric interactions between hemin and Ag NPs measured in the absorption spectra; see Supporting Information, Figure S3). However, only when the laser frequency matches the energy difference between the metallic Fermi level and molecular LUMO does the charge-transfer term in the SERS enhancement start to become a prominent factor. Although ground-state charge transfer may also make a minor contribution to the SERS enhancement, the signal enhancement is probably not detectable without additional electromagnetic enhancement.[90]

The thermal fluctuation-induced single-electron redox reaction at the molecule−metal interface is most likely a general phenomenon if the molecule has energetically accessible orbitals in terms of the metal Fermi level. This concept has been further demonstrated by using electrochemical STM to adjust the Fermi level of the metal substrate and directly monitor the molecule oxidation state change by nanoscale imaging (Figure.7). As a control experiment, Co(II) phthalocyanine (CoPc), which has a molecular structure quite similar to that of hemin but has a much flatter molecular structure for an STM study, is investigated in real time to probe the single-molecule redox reaction. As shown in Figure 7, under a reduction potential of 0.1 V_{SCE} (the reduction peak is located at 0.15 V_{SCE} in cyclic voltammetry), some CoPc molecules show changes in their oxidation states indicated by the bright−dark switching of their image contrast. The bright−dark switching of molecular imaging contrast implies that the d_{z^2} orbital of Co^{2+} releases or captures one additional electron from the Au substrate in nature. This is consistent with previous reports on other molecules.[91,92] Here, we note that the possibility of molecule adsorption−desorption as a cause for contrast change is ruled out because the pits in the molecular matrix are not completely empty, i.e., the faded contrast is due to molecule oxidation state change but not to molecule dissociation from the sites.

SMSERS-combined single-molecule spectroelectrochemistry presented here is a unique technique for probing the single-molecule charge transfer events and dynamics at the molecule−metal interface without an applied biased potential. If this

technique is combined with AFM/STM measurements, such as our reported site-specific AFM-correlated Raman spectroscopy,[31,70,93] it will have high spatial resolution, be more powerful, and can be applied to many other research fields such as photocatalysis and bioremediation. On the other hand, although it is difficult to probe the ultrafast dynamics at the single-molecule level, if this approach is combined with ensemble-averaged femtosecond stimulated Raman spectroscopy,[94] it may be able to obtain additional dynamical information such as high-resolution multidimensional structural information on the time scale of molecular vibrations (10 fs to 1 ps).

CONCLUSION

The ground-state single-electron charge transfer dynamics at the hemin−Ag NP interface has been investigated by using SMSERS and spectroelectrochemistry. The electron transfer at the hemin−Ag interface is evidenced by the prominent shift of a specific Raman mode, ν_4, which is a typical marker of the oxidation state of the iron center in hemin. The fluctuation dynamics of the Raman spectra has been quantitatively investigated by autocorrelation and cross-correlation function analysis. On the basis of the data analysis, combined with the single-molecule spectroelectrochemistry control measurements, we suggest that the single-molecule redox reaction at the hemin−Ag interface is primarily driven by thermal fluctuation. The ground-state single-electron charge transfer events at the hemin−Ag NP interface naturally exist, and they are different from the photodriven charge-transfer enhancement factor in SERS. This work reveals a real-time picture of the charge transfer dynamics at the molecule−metal interface without a strong electric field. Our new information is relevant for a further understanding, design, and manipulation of the charge transfer processes at molecule−metal interfaces or metal−molecule−metal junctions, which are fundamental elements in single-molecule electronics, catalysis, and solar energy conversion.

ASSOCIATED CONTENT

Supporting Information. Cross-correlation function curve (Figure S1), control experiment of changing laser excitation intensity (Figure S2), and an absorption spectrum (Figure S3). This material is available free of charge via the Internet at http://pubs.acs.org

AUTHOR INFORMATION

Corresponding Author
hplu@bgsu.edu

ACKNOWLEDGMENT

We acknowledge the support of this work from the Basic Energy Science of Department of Energy and the Division of Chemistry of National Science Foundation.

REFERENCES

(1) Defe ver, T.; Druet, M.; Rochelet-Dequaire, M.; Joannes, M.; Grossiord, C.; Limoges, B.; Marchal, D. *J. Am. Chem. Soc.* **2009**, *131*, 413–417.
(2) Tominaga, M.; Soejima, K.; Taniguchi, I. *J. Electroanal. Chem.* **2008**, *617*, 78–84.
(3) Kiwi, J.; Grätzel, M. *J. Am. Chem. Soc.* **1979**, *101*, 7214–7217.
(4) Shikanai, D.; Murase, H.; Hata, T.; Urabe, H. *J. Am. Chem. Soc.* **2009**, *131*, 3166–3167.
(5) Bakhmutsky, K.; Zhou, G.; Timothy, S.; Gorte, R. J. *Catal. Lett.* **2009**, *129*, 61–65.
(6) Murakami, N.; Chiyoya, T.; Tsubota, T.; Ohno, T. *Appl. Catal., A* **2008**, *348*, 148–152.
(7) Uchida, T.; Mogami, H.; Yamakata, A.; Sasaki, Y.; Osawa, M. *J. Am. Chem. Soc.* **2008**, *130*, 10862–10863.
(8) Lima, P. R.; Santos, W. J.; de Oliveira, A. B.; Goulart, M. O.; Kubota, L. T. *Biosens. Bioelectron.* **2008**, *24*, 448–454.
(9) Moser, C. C.; Dutton, P. L. *Biochemistry* **1988**, *27*, 2450–2461.
(10) Krol, M.; Ivanov, A. G.; Booij-James, I.; Mattoo, A. K.; Sane, P. V.; Huner, N. *Biochem. Cell Biol.* **2009**, *87*, 557–566.
(11) Aviram, A.; Ratner, M. A. *Chem. Phys. Lett.* **1974**, *29*, 277–283.
(12) Moth-Poulsen, K.; Bjørnholm, T. *Nat. Nano.* **2009**, *4*, 551–556.
(13) Kihira, Y.; Shimada, T.; Matsuo, Y.; Nakamura, E.; Hasegawa, T. *Nano Lett.* **2009**, *9*, 1442–1446.
(14) Taniguchi, M.; Tsutsui, M.; Shoji, K.; Fujiwara, H.; Kawai, T. *J. Am. Chem. Soc.* **2009**, *131*, 14146–14147.
(15) Selzer, Y.; Allara, D. L. *Annu. Rev. Phys. Chem.* **2006**, *57*, 593–623.
(16) Martín, S. *J. Phys. Chem. C* **2009**, *113*, 18884–18890.
(17) Reed, M. A.; Zhou, C.; Muller, C. J.; Burgin, T. P.; Tour, J. M. *Science* **1997**, *278*, 252–254.
(18) Bumm, L. A.; Arnold, J. J.; Cygan, M. T.; Dunbar, T. D.; Burgin, T. P.; Jones, L.; Allara, D. L.; Tour, J. M.; Weiss, P. S. *Science* **1996**, *271*, 1705–1707.
(19) Joachim, C.; Gimzewski, J. K.; Schlittler, R. R.; Chavy, C. *Phys. Rev. Lett.* **1995**, *74*, 2102–2105.
(20) Chen, F.; Hihath, J.; Huang, Z.; Li, X.; Tao, N. J. *Annu. Rev. Phys. Chem.* **2007**, *58*, 535–564.
(21) Tao, N. J. *Phys. Rev. Lett.* **1996**, *76*, 4066–4069.
(22) Park, H.; Park, J.; Lim, A. K. L.; Anderson, E. H.; Alivisatos, A. P.; McEuen, P. L. *Nature* **2000**, *407*, 57–60.
(23) Tao, N. J. *Nat. Nano.* **2006**, *1*, 173–181.
(24) Chen, F.; Tao, N. J. *Acc. Chem. Res.* **2009**, *42*, 429–438.
(25) Ambrose, W. P.; Moerner, W. E. *Nature* **1991**, *349*, 225–227.
(26) Bout, D. A. V.; Yip, W. T.; Hu, D.; Fu, D. K.; Swager, T. M.; Barbara, P. F. *Science* **1997**, *277*, 1074–1077.
(27) Lu, H. P.; Xie, X. S. *Nature* **1997**, *385*, 143–146.
(28) Xie, X. S.; Dunn, R. C. *Science* **1994**, *265*, 361–364.
(29) Lu, H. P.; Xun, L. Y.; Xie, X. S. *Science* **1998**, *282*, 1877–1882.
(30) Lu, H. P.; Xie, X. S. *J. Phys. Chem. B* **1997**, *101*, 2753–2757.
(31) Lu, H. P. *J. Phys.: Condens. Matter* **2005**, *17*, R333–R355.
(32) Lu, H. P. *Acc. Chem. Res.* **2005**, *38*, 557–565.
(33) Biju, V.; Micic, M.; Hu, D.; Lu, H. P. *J. Am. Chem. Soc.* **2004**, *126*, 9374–9381.
(34) Wang, Y.; Wang, X.; Ghosh, S. K.; Lu, H. P. *J. Am. Chem. Soc.* **2009**, *131*, 1479–1487.
(35) Wang, Y. M.; Wang, X. F.; Lu, H. P. *J. Am. Chem. Soc.* **2009**, *131*, 9020–9025.
(36) Pan, D.; Hu, D.; Lu, H. P. *J. Phys. Chem. B* **2005**, *109*, 16390–16395.
(37) Guo, L. J.; Wang, Y. M.; Lu, H. P. *J. Am. Chem. Soc.* **2010**, *132*, 1999–2004.
(38) Issac, A.; Jin, S.; Lian, T. *J. Am. Chem. Soc.* **2008**, *130*, 11280–11281.
(39) Cui, S. C.; Tachikawa, T.; Fujitsuka, M.; Majima, T. *J. Phys. Chem. C* **2008**, *112*, 19625–19634.
(40) Xu, W.; Kong, J. S.; Yeh, Y. T. E.; Chen, P. *Nat. Mater.* **2008**, *7*, 992–996.
(41) Li, S. C.; Chu, L. N.; Gong, X. Q.; Diebold, U. *Science* **2010**, *328*, 882–884.
(42) Lee, P. C.; Meisel, D. *J. Phys. Chem.* **1982**, *86*, 3391–3395.
(43) Nie, S. M.; Emery, S. R. *Science* **1997**, *275*, 1102–1106.
(44) Wustholz, K. L.; Henry, A. I.; McMahon, J. M.; Freeman, R. G.; Valley, N.; Piotti, M. E.; Natan, M. J.; Schatz, G. C.; Duyne, R. P. V. *J. Am. Chem. Soc.* **2010**, *132*, 10903–10910.

(45) Michaels, A. M.; Nirmal, M.; Brus, L. E. *J. Am. Chem. Soc.* **1999**, *121*, 9932–9939.
(46) Sanchez, L. A.; Spiro, T. G. *J. Phys. Chem.* **1985**, *89*, 763–768.
(47) Cai, W. B.; Stefan, I. C.; Scherson, D. A. *J. Electroanal. Chem.* **2002**, *524*, 36–42.
(48) Mcmahon, J. J.; Baer, S.; Melendres, C. A. *J. Phys. Chem.* **1986**, *90*, 1572–1577.
(49) Bizzarri, A. R.; Cannistraro, S. *Chem. Phys. Lett.* **2004**, *395*, 222–226.
(50) Bizzarri, A. R.; Cannistraro, S. *Chem. Phys.* **2003**, *290*, 297–306.
(51) Feng, M.; Tachikawa, H. *J. Am. Chem. Soc.* **2008**, *130*, 7443–7448.
(52) Abe, M.; Kitagawa, T.; Kyogoku, Y. *J. Chem. Phys.* **1978**, *69*, 4526–4534.
(53) Kneipp, K.; Wang, Y.; Kneipp, H.; Perelman, L. T.; Itzkan, I.; Dasari, R.; Feld, M. S. *Phys. Rev. Lett.* **1997**, *78*, 1667–1670.
(54) Dieringer, J. A.; Wustholz, K. L.; Masiello, D. J.; Camden, J. P.; Kleinman, S. L.; Schatz, G. C.; Van Duyne, R. P. *J. Am. Chem. Soc.* **2009**, *131*, 849–854.
(55) Xu, H. X.; Bjerneld, E. J.; Kall, M.; Borjesson, L. *Phys. Rev. Lett.* **1999**, *83*, 4357–4360.
(56) Bizzarri, A. R.; Cannistraro, S. *Phys. Rev. Lett.* **2005**, *94*, 068313-1–068313-4.
(57) Weiss, A.; Haran, G. *J. Phys. Chem. B* **2001**, *105*, 12348–12354.
(58) Meixner, A. J.; Vosgrone, T.; Sackrow, M. *J. Lumin.* **2001**, *94*, 147–152.
(59) Wang, Z. J.; Rothberg, L. J. *J. Phys. Chem. B* **2005**, *109*, 3387–3391.
(60) Le Ru, E. C.; Meyer, M.; Etchegoin, P. G. *J. Phys. Chem. B* **2006**, *110*, 1944–1948.
(61) Moore, A. A.; Jacobson, M. L.; Belabas, N.; Rowlen, K. L.; Jonas, D. M. *J. Am. Chem. Soc.* **2005**, *127*, 7292–7293.
(62) Walter, M. J.; Borys, N. J.; Gaefke, G.; Hoger, S.; Lupton, J. M. *J. Am. Chem. Soc.* **2008**, *130*, 16830–16831.
(63) Habuchi, S.; Cotlet, M.; Gronheid, R.; Dirix, G.; Michiels, J.; Vanderleyden, J.; De Schryver, F. C.; Hofkens, J. *J. Am. Chem. Soc.* **2003**, *125*, 8446–8447.
(64) Vosgröne, T.; Meixner, A. *ChemPhysChem* **2005**, *6*, 154–163.
(65) Lukatsky, D. B.; Haran, G.; Safran, S. A. *Phys. Rev. E* **2003**, *67*, 062402-1 −062402-4.
(66) Blackie, E. J.; Le Ru, E. C.; Etchegoin, P. G. *J. Am. Chem. Soc.* **2009**, *131*, 14466–14472.
(67) Etchegoin, P. G.; Le Ru, E. C. *Anal. Chem.* **2010**, *82*, 2888–2892.
(68) Haran, G. *Isr. J. Chem.* **2004**, *44*, 385–390.
(69) Bosnick, K. A.; Jiang, J.; Brus, L. E. *J. Phys. Chem. B* **2002**, *106*, 8096–8099.
(70) Suh, Y. D.; Schenter, G. K.; Zhu, L. Y.; Lu, H. P. *Ultramicroscopy* **2003**, *97*, 89–102.
(71) Luo, Z. X.; Luo, Y.; Li, J.; Liu, K.; Fu, H. B.; Ma, Y.; Yao, J. N. *Chem. Commun.* **2009**, *11*, 1342–1344.
(72) Stracke, F.; Blum, C.; Becker, S.; Müllen, K.; Meixner, A. *Chem. Phys. Lett.* **2000**, *325*, 196–202.
(73) We note that the Raman signals of the intermediate states are not from a time-averaged effect because the single electron transfer events can be time-resolved on a 20 s time scale as evidenced in Figure 2A.
(74) Vitali, L.; Levita, G.; Ohmann, R.; Comisso, A.; De Vita, A.; Kern, K. *Nat. Mater.* **2010**, *9*, 320–323.
(75) Leung, T. C.; Kao, C. L.; Su, W. S.; Feng, Y. J.; Chan, C. T. *Phys. Rev. B* **2003**, *68*, 195408-1−195408-6.
(76) Tseng, T. C.; Urban, C.; Wang, Y.; Otero, R.; Tait, S. L.; Alcam, M.; Écija, D.; Trelka, M.; Gallego, J. M.; Lin, N. *Nat. Chem.* **2010**, *2*, 374–379.
(77) Romaner, L.; Heimel, G.; Brédas, J. L.; Gerlach, A.; Schreiber, F.; Johnson, R. L.; Zegenhagen, J.; Duhm, S.; Koch, N.; Zojer, E. *Phys. Rev. Lett.* **2007**, *99*, 256801-1−256801-4.
(78) Ziroff, J.; Forster, F.; Schöll, A.; Puschnig, P.; Reinert, F. *Phys. Rev. Lett.* **2010**, *104*, 233004-1−233004-4.
(79) Degroot, J.; Hester, R. E. *J. Phys. Chem.* **1987**, *91*, 1693–1696.
(80) Wang, X. F.; Lu, H. P. *J. Phys. Chem. B* **2008**, *112*, 14920–14926.
(81) Ayars, E.; Hallen, H.; Jahncke, C. *Phys. Rev. Lett.* **2000**, *85*, 4180–4183.
(82) Livshits, E.; Baer, R.; Kosloff, R. *J. Phys. Chem. A* **2009**, *113*, 7521–7527.
(83) Palacios, R. E.; Fan, F. R. F.; Bard, A. J.; Barbara, P. F. *J. Am. Chem. Soc.* **2006**, *128*, 9028–9029.
(84) Lei, C.; Hu, D.; Ackerman, E. J. *Chem. Commun.* **2008**, *2008*, 5490–5492.
(85) Shegai, T.; Vaskevich, A.; Rubinstein, I.; Haran, G. *J. Am. Chem. Soc.* **2009**, *131*, 14390–14398.
(86) Ly, H. K.; Marti, M. A.; Martin, D. F.; Alvarez-Paggi, D.; Meister, W.; Kranich, A.; Weidinger, I. M.; Hildebrandt, P.; Murgida, D. H. *ChemPhysChem* **2010**, *11*, 1225–1235.
(87) Rahav, S.; Mukamel, S. *J. Chem. Phys.* **2010**, *133*, 244106-1−244106-12.
(88) Lombardi, J. R.; Birke, R. L. *J. Phys. Chem. C* **2008**, *112*, 5605–5617.
(89) Brus, L. *Acc. Chem. Res.* **2008**, *41*, 1742–1749.
(90) Lippitsch, M. *Phys. Rev. B* **1984**, *29*, 3101–3110.
(91) He, Y.; Borguet, E. *Angew. Chem., Int. Ed.* **2007**, *46*, 6098–6101.
(92) Comanici, K.; Buchner, F.; Flechtner, K.; Lukasczyk, T.; Gottfried, J. M.; Steinruck, H. P.; Marbach, H. *Langmuir* **2008**, *24*, 1897–1901.
(93) Pan, D. H.; Klymyshyn, N.; Hu, D. H.; Lu, H. P. *Appl. Phys. Lett.* **2006**, *88*, 093121-1−093121-3.
(94) Fang, C.; Frontiera, R. R.; Tran, R.; Mathies, R. A. *Nature* **2009**, *462*, 200–204.